

Spin-Parity Analysis of $p\bar{p}$ Mass Threshold Structure in J/ψ and ψ' Radiative Decays

M. Ablikim¹, M. N. Achasov⁵, D. Alberto⁴¹, D.J. Ambrose³⁸, F. F. An¹, Q. An³⁹, Z. H. An¹, J. Z. Bai¹, R. B. F. Baldini Ferroli¹⁷, Y. Ban²⁵, J. Becker², N. Berger¹, M. B. Bertani¹⁷, J. M. Bian¹, E. Boger^{18a}, O. Bondarenko¹⁹, I. Boyko¹⁸, R. A. Briere³, V. Bytev¹⁸, X. Cai¹, A. C. Calcaterra¹⁷, G. F. Cao¹, J. F. Chang¹, G. Chelkov^{18a}, G. Chen¹, H. S. Chen¹, J. C. Chen¹, M. L. Chen¹, S. J. Chen²³, Y. Chen¹, Y. B. Chen¹, H. P. Cheng¹³, Y. P. Chu¹, D. Cronin-Hennessy³⁷, H. L. Dai¹, J. P. Dai¹, D. Dedovich¹⁸, Z. Y. Deng¹, I. Denysenko^{18b}, M. Destefanis⁴¹, W. L. Ding Ding²⁷, Y. Ding²¹, L. Y. Dong¹, M. Y. Dong¹, S. X. Du⁴⁴, J. Fang¹, S. S. Fang¹, C. Q. Feng³⁹, C. D. Fu¹, J. L. Fu²³, Y. Gao³⁴, C. Geng³⁹, K. Goetzen⁷, W. X. Gong¹, M. Greco⁴¹, M. H. Gu¹, Y. T. Gu⁹, Y. H. Guan⁶, A. Q. Guo²⁴, L. B. Guo²², Y.P. Guo²⁴, Y. L. Han¹, X. Q. Hao¹, F. A. Harris³⁶, K. L. He¹, M. He¹, Z. Y. He²⁴, Y. K. Heng¹, Z. L. Hou¹, H. M. Hu¹, J. F. Hu⁶, T. Hu¹, B. Huang¹, G. M. Huang¹⁴, J. S. Huang¹¹, X. T. Huang²⁷, Y. P. Huang¹, T. Hussain⁴⁰, C. S. Ji³⁹, Q. Ji¹, X. B. Ji¹, X. L. Ji¹, L. K. Jia¹, L. L. Jiang¹, X. S. Jiang¹, J. B. Jiao²⁷, Z. Jiao¹³, D. P. Jin¹, S. Jin¹, F. F. Jing³⁴, N. Kalantar-Nayestanaki¹⁹, M. Kavatsyuk¹⁹, W. Kuehn³⁵, W. Lai¹, J. S. Lange³⁵, J. K. C. Leung³³, C. H. Li¹, Cheng Li³⁹, Cui Li³⁹, D. M. Li⁴⁴, F. Li¹, G. Li¹, H. B. Li¹, J. C. Li¹, K. Li¹⁰, Lei Li¹, N. B. Li²², Q. J. Li¹, S. L. Li¹, W. D. Li¹, W. G. Li¹, X. L. Li²⁷, X. N. Li¹, X. Q. Li²⁴, X. R. Li²⁶, Z. B. Li³¹, H. Liang³⁹, Y. F. Liang²⁹, Y. T. Liang³⁵, G. R. Liao³⁴, X. T. Liao¹, B. J. Liu³², C. L. Liu³, C. X. Liu¹, C. Y. Liu¹, F. H. Liu²⁸, Fang Liu¹, Feng Liu¹⁴, H. Liu¹, H. B. Liu⁶, H. H. Liu¹², H. M. Liu¹, H. W. Liu¹, J. P. Liu⁴², K. Liu²⁵, K. Liu⁶, K. Y. Liu²¹, Q. Liu³⁶, S. B. Liu³⁹, X. Liu²⁰, X. H. Liu¹, Y. B. Liu²⁴, Yong Liu¹, Z. A. Liu¹, Zhiqiang Liu¹, Zhiqing Liu¹, H. Loehner¹⁹, G. R. Lu¹¹, H. J. Lu¹³, J. G. Lu¹, Q. W. Lu²⁸, X. R. Lu⁶, Y. P. Lu¹, C. L. Lu²², M. X. Luo⁴³, T. Luo³⁶, X. L. Luo¹, M. Lv¹, C. L. Ma⁶, F. C. Ma²¹, H. L. Ma¹, Q. M. Ma¹, S. Ma¹, T. Ma¹, X. Y. Ma¹, M. Maggiora⁴¹, Q. A. Malik⁴⁰, H. Mao¹, Y. J. Mao²⁵, Z. P. Mao¹, J. G. Messchendorp¹⁹, J. Min¹, T. J. Min¹, R. E. Mitchell¹⁶, X. H. Mo¹, N. Yu. Muchnoi⁵, Y. Nefedov¹⁸, I. B. Nikolaev⁵, Z. Ning¹, S. L. Olsen²⁶, Q. Ouyang¹, S. P. Pacetti^{17c}, J. W. Park²⁶, M. Pelizaeus³⁶, K. Peters⁷, J. L. Ping²², R. G. Ping¹, R. Poling³⁷, C. S. J. Pun³³, M. Qi²³, S. Qian¹, C. F. Qiao⁶, X. S. Qin¹, J. F. Qiu¹, K. H. Rashid⁴⁰, G. Rong¹, X. D. Ruan⁹, A. Sarantsev^{18d}, J. Schulze², M. Shao³⁹, C. P. Shen^{36e}, X. Y. Shen¹, H. Y. Sheng¹, M. R. Shepherd¹⁶, X. Y. Song¹, S. Spataro⁴¹, B. Spruck³⁵, D. H. Sun¹, G. X. Sun¹, J. F. Sun¹¹, S. S. Sun¹, X. D. Sun¹, Y. J. Sun³⁹, Y. Z. Sun¹, Z. J. Sun¹, Z. T. Sun³⁹, C. J. Tang²⁹, X. Tang¹, E. H. Thorndike³⁸, H. L. Tian¹, D. Toth³⁷, G. S. Varner³⁶, B. Wang⁹, B. Q. Wang²⁵, K. Wang¹, L. L. Wang⁴, L. S. Wang¹, M. Wang²⁷, P. Wang¹, P. L. Wang¹, Q. Wang¹, Q. J. Wang¹, S. G. Wang²⁵, X. F. Wang¹¹, X. L. Wang³⁹, Y. D. Wang³⁹, Y. F. Wang¹, Y. Q. Wang²⁷, Z. Wang¹, Z. G. Wang¹, Z. Y. Wang¹, D. H. Wei⁸, Q.G. Wen³⁹, S. P. Wen¹, U. Wiedner², L. H. Wu¹, N. Wu¹, W. Wu²⁴, Z. Wu¹, Z. J. Xiao²², Y. G. Xie¹, Q. L. Xiu¹, G. F. Xu¹, G. M. Xu²⁵, H. Xu¹, Q. J. Xu¹⁰, X. P. Xu³⁰, Y. Xu²⁴, Z. R. Xu³⁹, Z. Xue¹, L. Yan³⁹, W. B. Yan³⁹, Y. H. Yan¹⁵, H. X. Yang¹, T. Yang⁹, Y. Yang¹⁴, Y. X. Yang⁸, H. Ye¹, M. Ye¹, M.H. Ye⁴, B. X. Yu¹, C. X. Yu²⁴, S. P. Yu²⁷, C. Z. Yuan¹, W. L. Yuan²², Y. Yuan¹, A. A. Zafar⁴⁰, A. Z. Zallo¹⁷, Y. Zeng¹⁵, B. X. Zhang¹, B. Y. Zhang¹, C. C. Zhang¹, D. H. Zhang¹, H. H. Zhang³¹, H. Y. Zhang¹, J. Zhang²², J. Q. Zhang¹, J. W. Zhang¹, J. Y. Zhang¹, J. Z. Zhang¹, L. Zhang²³, S. H. Zhang¹, T. R. Zhang²², X. J. Zhang¹, X. Y. Zhang²⁷, Y. Zhang¹, Y. H. Zhang¹, Y. S. Zhang⁹, Z. P. Zhang³⁹, Z. Y. Zhang⁴², G. Zhao¹, H. S. Zhao¹, Jingwei Zhao¹, Lei Zhao³⁹, Ling Zhao¹, M. G. Zhao²⁴, Q. Zhao¹, S. J. Zhao⁴⁴, T. C. Zhao¹, X. H. Zhao²³, Y. B. Zhao¹, Z. G. Zhao³⁹, A. Zhemchugov^{18a}, B. Zheng¹, J. P. Zheng¹, Y. H. Zheng⁶, Z. P. Zheng¹, B. Zhong¹, J. Zhong², L. Zhou¹, X. K. Zhou⁶, X. R. Zhou³⁹, C. Zhu¹, K. Zhu¹, K. J. Zhu¹, S. H. Zhu¹, X. L. Zhu³⁴, X. W. Zhu¹, Y. S. Zhu¹, Z. A. Zhu¹, J. Zhuang¹, B. S. Zou¹, J. H. Zou¹, J. X. Zuo¹

(BESIII Collaboration)

¹ Institute of High Energy Physics, Beijing 100049, P. R. China

² Bochum Ruhr-University, 44780 Bochum, Germany

³ Carnegie Mellon University, Pittsburgh, PA 15213, USA

⁴ China Center of Advanced Science and Technology, Beijing 100190, P. R. China

⁵ G.I. Budker Institute of Nuclear Physics SB RAS (BINP), Novosibirsk 630090, Russia

⁶ Graduate University of Chinese Academy of Sciences, Beijing 100049, P. R. China

⁷ GSI Helmholtzcentre for Heavy Ion Research GmbH, D-64291 Darmstadt, Germany

⁸ Guangxi Normal University, Guilin 541004, P. R. China

⁹ GuangXi University, Nanning 530004, P.R. China

¹⁰ Hangzhou Normal University, XueLin Jie 16, Xiasha Higher Education Zone, Hangzhou, 310036

¹¹ Henan Normal University, Xinxiang 453007, P. R. China

¹² Henan University of Science and Technology,

¹³ Huangshan College, Huangshan 245000, P. R. China

¹⁴ Huazhong Normal University, Wuhan 430079, P. R. China

¹⁵ Hunan University, Changsha 410082, P. R. China

¹⁶ Indiana University, Bloomington, Indiana 47405, USA

¹⁷ INFN Laboratori Nazionali di Frascati, Frascati, Italy

¹⁸ Joint Institute for Nuclear Research, 141980 Dubna, Russia

¹⁹ KVI/University of Groningen, 9747 AA Groningen, The Netherlands

²⁰ Lanzhou University, Lanzhou 730000, P. R. China

²¹ Liaoning University, Shenyang 110036, P. R. China

²² Nanjing Normal University, Nanjing 210046, P. R. China

²³ Nanjing University, Nanjing 210093, P. R. China

- ²⁴ Nankai University, Tianjin 300071, P. R. China
²⁵ Peking University, Beijing 100871, P. R. China
²⁶ Seoul National University, Seoul, 151-747 Korea
²⁷ Shandong University, Jinan 250100, P. R. China
²⁸ Shanxi University, Taiyuan 030006, P. R. China
²⁹ Sichuan University, Chengdu 610064, P. R. China
³⁰ Soochow University, Suzhou 215006, China
³¹ Sun Yat-Sen University, Guangzhou 510275, P. R. China
³² The Chinese University of Hong Kong, Shatin, N.T., Hong Kong.
³³ The University of Hong Kong, Pokfulam, Hong Kong
³⁴ Tsinghua University, Beijing 100084, P. R. China
³⁵ Universitaet Giessen, 35392 Giessen, Germany
³⁶ University of Hawaii, Honolulu, Hawaii 96822, USA
³⁷ University of Minnesota, Minneapolis, MN 55455, USA
³⁸ University of Rochester, Rochester, New York 14627, USA
³⁹ University of Science and Technology of China, Hefei 230026, P. R. China
⁴⁰ University of the Punjab, Lahore-54590, Pakistan
⁴¹ University of Turin and INFN, Turin, Italy
⁴² Wuhan University, Wuhan 430072, P. R. China
⁴³ Zhejiang University, Hangzhou 310027, P. R. China
⁴⁴ Zhengzhou University, Zhengzhou 450001, P. R. China

^a also at the Moscow Institute of Physics and Technology, Moscow, Russia

^b on leave from the Bogolyubov Institute for Theoretical Physics, Kiev, Ukraine

^c Currently at University of Perugia and INFN, Perugia, Italy

^d also at the PNPI, Gatchina, Russia

^e now at Nagoya University, Nagoya, Japan

(Dated: December 6, 2011)

A partial wave analysis of the $p\bar{p}$ mass-threshold enhancement in the reaction $J/\psi \rightarrow \gamma p\bar{p}$ is used to determine: its J^{PC} quantum numbers to be 0^{-+} ; its peak mass to be below threshold at $M = 1832_{-5}^{+19}$ (stat.) $_{-17}^{+18}$ (syst.) ± 19 (model) MeV/ c^2 ; and its total width to be $\Gamma < 76$ MeV/ c^2 at the 90% C.L. The product branching ratio is measured to be $B(J/\psi \rightarrow \gamma X(p\bar{p}))B(X(p\bar{p}) \rightarrow p\bar{p}) = (9.0_{-1.1}^{+0.4}$ (stat.) $_{-5.0}^{+1.5}$ (syst.) ± 2.3 (model)) $\times 10^{-5}$. A similar analysis performed on $\psi' \rightarrow \gamma p\bar{p}$ decays shows, for the first time, the presence of a corresponding enhancement with a production rate relative to that for J/ψ decays of $R = (5.08_{-0.45}^{+0.71}$ (stat.) $_{-3.58}^{+0.67}$ (syst.) ± 0.12 (model)) %.

PACS numbers: 12.39.Mk, 12.40.Yx, 13.20.Gd, 13.75.Cs

An anomalously strong $p\bar{p}$ mass threshold enhancement was first observed by the BESII experiment in the radiative decay process $J/\psi \rightarrow \gamma p\bar{p}$ [1] and was recently confirmed by the BESIII and CLEO-c [2] experiments. Curiously, no apparent corresponding structures were seen in near-threshold $p\bar{p}$ cross section measurements, in B -meson decays [3], in radiative ψ' or $\Upsilon \rightarrow \gamma p\bar{p}$ decays [4], or in $J/\psi \rightarrow \omega p\bar{p}$ decays [5]. These non-observations disfavor the mass-threshold enhancement attribution to the effects of $p\bar{p}$ final state interactions (FSI) [6–8].

A number of theoretical speculations have been proposed to interpret the nature of this structure [6–10]. Among them, one intriguing suggestion is that it is due to a $p\bar{p}$ bound state, sometimes called baryonium [10], an object with a long history and the subject of many experimental searches [11]. The observation of the $p\bar{p}$ mass threshold enhancement also stimulated an experimental analysis of $J/\psi \rightarrow \gamma\pi^+\pi^-\eta'$ decays, in which a $\pi^+\pi^-\eta'$ resonance, the $X(1835)$, was first observed by the BESII experiment [12] and recently confirmed with high statistical significance by the BESIII experiment [13].

Whether or not the $p\bar{p}$ mass threshold enhancement and the $X(1835)$ are related to the same source still needs further study; among these, spin-parity determinations and precise measurements of the masses, widths and branching ratios are especially important.

In this letter, we report the first partial wave analysis (PWA) of the $p\bar{p}$ mass threshold structure produced via the decays of $J/\psi \rightarrow \gamma p\bar{p}$ and $\psi' \rightarrow \gamma p\bar{p}$. Data samples containing $(225.2 \pm 2.8) \times 10^6$ J/ψ events and $(106 \pm 4) \times 10^6$ ψ' events [14] accumulated in the Beijing Spectrometer (BESIII) [15] located at the Beijing Electron-Positron Collider (BEPCCII) [16] are used.

The cylindrical core of the BESIII detector consists of a helium-gas-based drift chamber (MDC), a plastic scintillator Time-of-Flight system (TOF), and a CsI(Tl) Electromagnetic Calorimeter (EMC), all enclosed in a superconducting solenoidal magnet that provides a 1.0-T magnetic field. The solenoid is supported by an octagonal flux-return yoke with resistive plate counter muon identifier modules (MU) interleaved with steel plates. The solid angle for the charged particle and photon acceptance is 93% of 4π , and the charged particle momentum

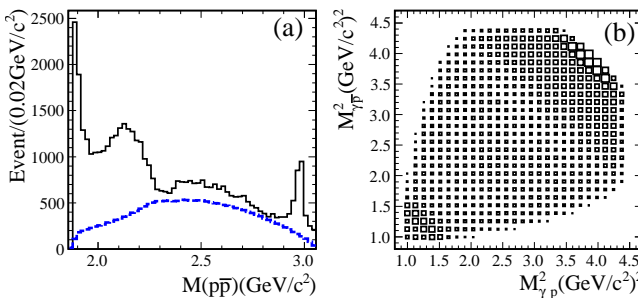


FIG. 1: The $p\bar{p}$ invariant mass spectrum for the selected $J/\psi \rightarrow \gamma p\bar{p}$ candidate events. (a) The $p\bar{p}$ invariant mass spectrum; the open histogram is data and the dashed line is from $J/\psi \rightarrow \gamma p\bar{p}$ phase-space MC events (with arbitrary normalization). (b) An $M^2(\gamma p)$ (horizontal) versus $M^2(\gamma \bar{p})$ (vertical) Dalitz plot for the selected events.

and photon energy resolutions at 1 GeV are 0.5% and 2.5%, respectively. The time resolution of TOF is 80 ps in the barrel and 110 ps in the endcaps, and the dE/dx resolution is 6%.

Charged-particle tracks in the polar angle range $|\cos\theta| < 0.93$ are reconstructed from hits in the MDC. The TOF and dE/dx information are combined to form particle identification confidence levels for the π , K and p hypotheses; the particle type with the highest confidence level is assigned to each track. Photon candidates are required to have an energy deposit of at least 25 MeV in the barrel EMC ($|\cos\theta| < 0.8$) and 50 MeV in the endcap EMCs ($0.86 < |\cos\theta| < 0.92$), and be isolated from antiprotons by more than 30° .

Candidate $J/\psi \rightarrow \gamma p\bar{p}$ events are required to have at least one photon and two charged tracks identified as a proton and an antiproton. Requirements of $|U_{miss}| < 0.05$ GeV, where $U_{miss} = (E_{miss} - |P_{miss}|)$, and $P_{t\gamma}^2 < 0.0005$ $(\text{GeV}/c)^2$, where $P_{t\gamma}^2 = 4|P_{miss}|^2 \sin^2\theta_\gamma/2$, are imposed to suppress backgrounds from multi-photon events. Here E_{miss} and P_{miss} are, respectively, the missing energy and momentum of all charged particles, and θ_γ is the angle between the missing momentum and the photon direction. A four-constraint (4C) energy-momentum conservation kinematic fit is performed to the $\gamma p\bar{p}$ hypothesis. For events with more than one photon candidates, the combination with the minimum χ^2 is used; $\chi^2 < 20$ is also required. Since there are differences in detection efficiency between data and Monte Carlo (MC) simulated low-momentum tracks, we reject events containing any tracks with momentum below 0.3 GeV/c .

The $p\bar{p}$ mass spectrum for events that satisfy all of the above-listed criteria is shown in Fig. 1(a). There is a clear signal of η_c , a broad enhancement around $M_{p\bar{p}} \sim 2.1 \text{ GeV}/c^2$, and a prominent and narrow low-mass peak at the $p\bar{p}$ mass threshold, consistent with that reported by BESII [1] and BESIII [2]. The Dalitz plot for selected events is shown in Fig. 1(b).

Potential background processes are studied with an inclusive MC sample of $2 \times 10^8 J/\psi$ events generated

according to the Lund model [17]. None of the background sources produces an enhancement at the $p\bar{p}$ mass threshold region. The dominant background is from $J/\psi \rightarrow \pi^0 p\bar{p}$ events, with asymmetric $\pi^0 \rightarrow \gamma\gamma$ decays where one of the photons has most of the π^0 energy. An exclusive MC sample, generated according to the PWA results of $J/\psi \rightarrow \pi^0 p\bar{p}$ at BESII [18], indicates that the level of this background in the selected data sample with $M_{p\bar{p}} < 2.2 \text{ GeV}/c^2$ is 3.7% of the total. The $J/\psi \rightarrow \pi^0 p\bar{p}$ decay channel is also studied with data, and there is no evidence of a $p\bar{p}$ mass threshold enhancement, which provides further evidence that the enhancement observed in J/ψ decays is not from background.

A PWA of the events with $M_{p\bar{p}} < 2.2 \text{ GeV}/c^2$ is performed to focus on determining the parameters of the $p\bar{p}$ mass threshold structure, which we denote as $X(p\bar{p})$. The maximum likelihood method applied in the fit uses a likelihood function that is constructed from $\gamma p\bar{p}$ signal amplitudes described by the relativistic covariant tensor amplitude method [19] and MC efficiencies. The background contribution from the $\pi^0 p\bar{p}$ process is removed by subtracting the log-likelihood values of background events from that of data, since the log-likelihood value of data is the sum of the log-likelihood values of signal and background events [20]. Here, the background events are estimated by the MC sample of $J/\psi \rightarrow \pi^0 p\bar{p}$ decays described above. We include the effect of FSI in the PWA fit using the Julich formulation [6].

Four components, the $X(p\bar{p})$, $f_2(1910)$, $f_0(2100)$ and 0^{++} phase space (PS) are included in the PWA fit. The intermediate resonances are described by Breit-Wigner (BW) propagators, and the parameters of the $f_2(1910)$ and $f_0(2100)$ are fixed at PDG values. In the optimal PWA fit, the $X(p\bar{p})$ is assigned to be a 0^{-+} state. The statistical significance of the $X(p\bar{p})$ component of the fit is much larger than 30σ ; those for the other components are larger than 5σ , where the statistical significance is determined from the changes of likelihood value and degrees of freedom in the PWA fits with and without the signal hypotheses. The mass, width and product branching ratio (BR) of the $X(p\bar{p})$ are measured to be: $M = 1832^{+19}_{-5} \text{ MeV}/c^2$, $\Gamma = 13 \pm 39 \text{ MeV}/c^2$ and $B(J/\psi \rightarrow X)B(X \rightarrow p\bar{p}) = (9.0^{+0.4}_{-1.1}) \times 10^{-5}$, respectively, where the errors are statistical only. Figure 2 shows comparisons of the mass and angular distributions between the data and the PWA fit projections. For the spin-parity determination of the $X(p\bar{p})$, the 0^{-+} assignment fit is better than that for 0^{++} or other J^{PC} assignments with statistical significances that are larger than 6.8σ .

Variations of the fit included replacing the $f_0(2100)$ with the $f_2(2150)$, the $f_2(1910)$ with the $f_2(1950)$, and replacing both components simultaneously; changing the J^{PC} of the PS contribution, as well as consideration of the parameter uncertainties of the $f_0(2100)$ and $f_2(1910)$, were performed, and it is found the changes of the log-likelihood values and the parameters of the $X(p\bar{p})$ are quite small, except that when replacing 0^{++} PS with 0^{-+}

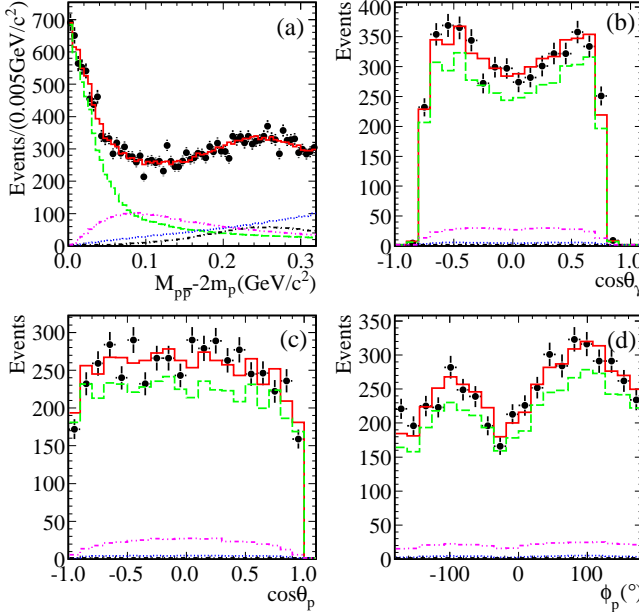


FIG. 2: Comparisons between data and PWA fit projection: (a) the $p\bar{p}$ invariant mass; (b)-(d) the polar angle θ_γ of the radiative photon in the J/ψ center of mass system, the polar angle θ_p and the azimuthal angle ϕ_p of the proton in the $p\bar{p}$ center of mass system with $M_{p\bar{p}} - 2m_p < 50 \text{ MeV}/c^2$, respectively. Here, the black dots with error bars are data, the solid histograms show the PWA total projection, and the dashed, dotted, dash-dotted and dash-dot-dotted lines show the contributions of the $X(p\bar{p})$, 0^{++} phase space, $f_0(2100)$ and $f_2(1910)$, respectively.

PS the event number of the $X(p\bar{p})$ decreases by 52%. We also tried fits that include other possible resonances listed in the PDG table [21] [$\eta_2(1870)$, $f_2(2010)$, $f_2(1950)$, $f_2(2150)$, $f_J(2220)$, $\eta(2225)$, $f_2(2300)$, $f_2(2340)$ etc.] as well as $X(2120)$ and $X(2370)$ [13], and different J^{PC} PS contributions. The statistical significances of these additional resonances are lower than 3σ . All of the parameter changes that are found in these alternative fits are considered as sources of systematic uncertainties.

For systematic errors on the mass and width of the $X(p\bar{p})$, in addition to those discussed above, we include uncertainties from different fit ranges of $M_{p\bar{p}} < 2.15 \text{ GeV}/c^2$ and $M_{p\bar{p}} < 2.25 \text{ GeV}/c^2$, different parameterizations for the BW formula, as well as different background levels. For the systematic errors of the BR measurement, there are additional uncertainties from the efficiencies of charged track detection, photon detection and particle identification, kinematic fit and the total number of J/ψ events. The total systematic errors on the mass and width of the $X(p\bar{p})$ are $+_{-17}^{+18} \text{ MeV}/c^2$ and $+_{-13}^{+10} \text{ MeV}/c^2$, respectively, and the corresponding relative systematic error on the product BR is $+_{-56}^{+17}\%$.

Various FSI models [6–8] have been proposed to interpret the $p\bar{p}$ mass threshold enhancement. Among them, a BW function times a one-pion-exchange FSI factor [8] can

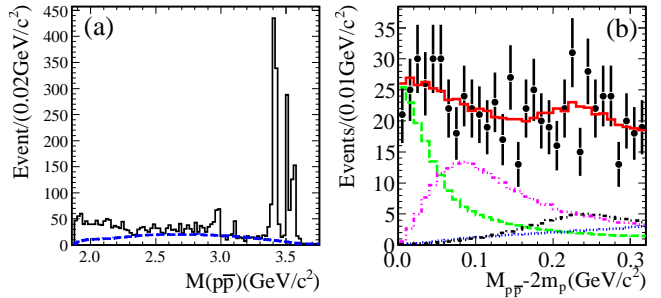


FIG. 3: (a) The $p\bar{p}$ invariant mass spectrum for the selected $\psi' \rightarrow \gamma p\bar{p}$ candidate events; the open histogram is data and the dashed line is from a $\psi' \rightarrow \gamma p\bar{p}$ phase-space MC events (with arbitrary normalization). (b) Comparisons between data and PWA fit projection for $p\bar{p}$ mass spectrum, the representations of the error bars and histograms are same as those in Fig. 2.

also describe the data well. For this case, the mass and width of the $X(p\bar{p})$ shift by 19 MeV/c^2 and 4 MeV/c^2 , respectively, while the relative change in the product BR is 25%. These errors are considered as second (model) systematic errors due to the uncertainty of the model dependence.

The $\psi' \rightarrow \gamma p\bar{p}$ decay channel is also studied using event selection criteria similar to those used in the $J/\psi \rightarrow \gamma p\bar{p}$ study. The $p\bar{p}$ mass spectrum of the surviving events is shown in Fig. 3(a). Besides the well known η_c and χ_{cJ} peaks, there is also a $p\bar{p}$ mass threshold excess relative to PS. However, here the line shape of the mass spectrum in the threshold region appears to be less pronounced than that in J/ψ decays. Potential background processes were extensively studied with an inclusive MC sample of $1 \times 10^8 \psi'$ events and a data sample of the selected $\psi' \rightarrow \pi^0 p\bar{p}$ events, and these indicate that the $p\bar{p}$ mass threshold structure is not from any background source. An exclusive MC sample, generated according to preliminary PWA results of $\psi' \rightarrow \pi^0 p\bar{p}$ decays with BE-SIII data [22], is applied to the background estimation, and the background level from this source in the selected data sample with $M_{p\bar{p}} < 2.2 \text{ GeV}/c^2$ is determined to be 3.4%.

A PWA on $\psi' \rightarrow \gamma p\bar{p}$ which is similar to that applied for $J/\psi \rightarrow \gamma p\bar{p}$ decays was performed to check the contribution of $X(p\bar{p})$ in ψ' decays and to measure the production ratio between J/ψ and ψ' radiative decays, $R = B(\psi' \rightarrow \gamma X(p\bar{p})) / B(J/\psi \rightarrow \gamma X(p\bar{p}))$. Due to limited statistics of ψ' events, in the PWA, the mass and width of $X(p\bar{p})$ as well as its J^{PC} were fixed to the results obtained from J/ψ decays. Figure 3(b) shows comparisons between data and MC projections for the $p\bar{p}$ mass spectrum. As in J/ψ decays, replacing the $f_0(2100)$ with the $f_2(2150)$ and the $f_2(1910)$ with the $f_2(1950)$ yields no significant change in fit quality. The determined product BR and R value are $B(\psi' \rightarrow \gamma X) \times B(X \rightarrow p\bar{p}) = (4.57 \pm 0.36) \times 10^{-6}$ and $R = (5.08^{+0.71}_{-0.45})\%$, respectively.

With the consideration of systematic uncertainties sim-

ilar to those in J/ψ decays, and the uncertainty of the total number of ψ' events, the total relative systematic error on the BR is $(^{+27}_{-89} \text{ (syst.)} \pm 28 \text{ (model)})\%$, and systematic error on R values is $(^{+0.67}_{-3.58} \text{ (syst.)} \pm 0.12 \text{ (model)})\%$. Similar to all cases studied in J/ψ analysis, the statistical significance of the $X(p\bar{p})$ is larger than 6.9σ in ψ' decays.

The PWA fits are also performed without the correction for FSI effect. The corresponding log-likelihood value worsen by 25.6 than those with FSI effect included. The mass, width and product BR of the $X(p\bar{p})$ are $M = 1861 \pm 1 \text{ (stat.)} ^{+13}_{-4} \text{ (syst.) MeV}/c^2$, $\Gamma = 1 \pm 6 \text{ (stat.)} ^{+18}_{-1} \text{ (syst.) MeV}/c^2$ (a total width of $\Gamma < 32 \text{ MeV}/c^2$ at the 90% C.L), $B(J/\psi \rightarrow \gamma X(1860))B(X(1860) \rightarrow p\bar{p}) = (8.6^{+0.3}_{-0.2} \text{ (stat.)} ^{+2.4}_{-3.5} \text{ (syst.)}) \times 10^{-5}$ and $B(\psi' \rightarrow \gamma X(1860))B(X(1860) \rightarrow p\bar{p}) = (4.15 \pm 0.39 \text{ (stat.)} ^{+2.51}_{-1.71} \text{ (syst.)}) \times 10^{-6}$, respectively. The corresponding R value is $(4.80^{+0.46}_{-0.48} \text{ (stat.)} ^{+2.24}_{-1.29} \text{ (syst.)})\%$.

In summary, the PWA of $J/\psi \rightarrow \gamma p\bar{p}$ and $\psi' \rightarrow \gamma p\bar{p}$ decays are performed. In J/ψ radiative decays, the near-threshold enhancement $X(p\bar{p})$ in the $p\bar{p}$ invariant mass is determined to be a 0^- state. With the inclusion of Julich-FSI effects, the mass, width and product BR for the $X(p\bar{p})$ are measured to be: $M = 1832^{+19}_{-5} \text{ (stat.)} ^{+18}_{-17} \text{ (syst.)} \pm 19 \text{ (model) MeV}/c^2$, $\Gamma = 13 \pm 39 \text{ (stat.)} ^{+10}_{-13} \text{ (syst.)} \pm 4 \text{ (model) MeV}/c^2$ (a total width of $\Gamma < 76 \text{ MeV}/c^2$ at the 90% C.L) and $B(J/\psi \rightarrow \gamma X)B(X \rightarrow p\bar{p}) = (9.0^{+0.4}_{-1.1} \text{ (stat.)} ^{+1.5}_{-5.0} \text{ (syst.)} \pm 2.3 \text{ (model)}) \times 10^{-5}$, respectively. The produce BR for $X(p\bar{p})$ in ψ' decay is first measured to be $B(\psi' \rightarrow$

$\gamma X) \times B(X \rightarrow p\bar{p}) = (4.57 \pm 0.36 \text{ (stat.)} ^{+1.23}_{-4.07} \text{ (syst.)} \pm 1.28 \text{ (model)}) \times 10^{-6}$ and the production ratio of the $X(p\bar{p})$ between J/ψ and ψ' radiative decays is $R = (5.08^{+0.71}_{-0.45} \text{ (stat.)} ^{+0.67}_{-3.58} \text{ (syst.)} \pm 0.12 \text{ (model)})\%$.

The mass of the $X(p\bar{p})$ measured in the PWA fit with FSI effect included is consistent with the $X(1835)$, but the width is significantly narrower. This indicates that either the $X(p\bar{p})$ and the $X(1835)$ come from different sources, or that interference effects in the $J/\psi \rightarrow \gamma\pi^+\pi^-\eta'$ process should not be ignored in the determination of the $X(1835)$ mass and width, or that there may be more than one resonance in the mass peak around 1.83 GeV/ c^2 in $J/\psi \rightarrow \gamma\pi^+\pi^-\eta'$ decays. When more J/ψ data are collected at BESIII, more sophisticated analyses, including a PWA, will be performed for the $J/\psi \rightarrow \gamma\pi\eta'$ decay channel. A measurement of the relative production ratios for the $X(1835)$ in J/ψ and ψ' radiative decays can further clarify on basis of their production ratios whether or not $X(p\bar{p})$ and $X(1835)$ are the same states.

We thank the accelerator group and computer staff of IHEP for their effort in producing beams and processing data. We are grateful for support from our institutes and universities and from these agencies: Ministry of Science and Technology of China, National Natural Science Foundation of China, Chinese Academy of Sciences, Istituto Nazionale di Fisica Nucleare, Russian Foundation for Basic Research, Russian Academy of Science (Siberian branch), U.S. Department of Energy, U.S. National Science Foundation, University of Groningen (RuG) and the Helmholtzzentrum fuer Schwerionenforschung GmbH (GSI), and National Research Foundation of Korea.

-
- [1] J.Z. Bai *et al.* (BES Collaboration), Phys. Rev. Lett. **91**, 022001 (2003).
 - [2] M. Ablikim *et al.* (BESIII Collaboration), Chin.Phys. **C34**, 421 (2010); J. P. Alexander *et al.* (CLEO Collaboration), Phys. Rev. **D 82**, 092002 (2010).
 - [3] S. Jin, Int. J. Mod. Phys. **A 20**, 5145 (2005); M.Z. Wang *et al.*, Phys. Rev. Lett. **92**, 131801 (2004).
 - [4] M. Ablikim *et al.* (BES Collaboration), Phys. Rev. Lett. **99**, 011802 (2007); S.B. Athar *et al.* (CLEO Collaboration), Phys. Rev. **D 73**, 032001 (2006).
 - [5] M. Ablikim *et al.* (BES Collaboration), Eur. Phys. J. **C53**, 15, (2008).
 - [6] A. Sirbirtsen *et al.*, Phys. Rev. **D 71**, 054010 (2005).
 - [7] G. Y. Chen *et al.*, Phys. Lett. **B 692**, 136 (2010).
 - [8] B. S. Zou and H. C. Chiang, Phys. Rev. **D 69**, 034004 (2003).
 - [9] X. H. Liu *et al.*, Phys. Rev. **D 80**, 034032 (2009); N. Kocherev and D. P. Min, Phys. Lett. **B 633**, 283 (2006); T. Huang and S. L. Zhu, Phys. Rev. **D 73**, 014023 (2006).
 - [10] A. Datta and P. J. O'Donnell, Phys. Lett. **B 567**, 273 (2003); M. L. Yan *et al.*, Phys. Rev. **D 72**, 034027 (2005); B. Loiseau *et al.*, Phys. Rev. **C 72**, 011001 (2005).
 - [11] E. Klempert *et al.*, Phys. Rep. **368**, 119 (2002).
 - [12] M. Ablikim *et al.* (BES Collaboration), Phys. Rev. Lett. **95**, 262001 (2005).
 - [13] M. Ablikim *et al.* (BESIII Collaboration), Phys. Rev. Lett. **106**, 072002 (2011).
 - [14] M. Ablikim *et al.* (BESIII Collaboration), Phys. Rev. **D 83**, 012003 (2011); **81**, 052005 (2010).
 - [15] M. Ablikim *et al.* (BESIII Collaboration), Nucl. Instrum. Meth. **A 614**, 345 (2010).
 - [16] J. Z. Bai *et al.* (BES Collaboration), Nucl. Instrum. Meth. **A 344**, 319 (1994); Nucl. Instrum. Meth. **A 458**, 627 (2001).
 - [17] J.C. Chen *et al.*, Phys. Rev. **D 62**, 034003 (2000).
 - [18] M. Ablikim *et al.* (BES Collaboration), Phys. Rev. **D 80**, 052004 (2009).
 - [19] S. Dulat and B. S. Zou, Eur. Phys. J. **A 26**, 125 (2005).
 - [20] M. Ablikim *et al.* (BES Collaboration), Phys. Lett. **B 598**, 149 (2004); **607**, 243 (2005); **633**, 681 (2006).
 - [21] K. Nakamura *et al.* (Particle Data Group), J. Phys. **G 37**, 075021 (2010).
 - [22] Y. Liang (for BESIII Collaboration), Proceedings of the 8th International Workshop on the Physics of Excited Nucleons (NSTAR2011), Newport News, May 17-20, 2011.